Power Stabilized Cryogenic Sapphire Oscillator

A. N. Luiten, A. G. Mann, M. E. Costa, and D. G. Blair

***Abstract*—Microwave oscillators of exceptional short-term stability have been realized from cryogenic sapphire resonators with loaded Q factors in excess of 10^9 at 11.9 GHz and 6K. This has been achieved by a power stabilized loop oscillator with active Pound frequency stabilization. These oscillators have exhibited a fractional frequency stability of 3–4$\times 10^{-15}$ for integration times from 0.3 to 100 s. The relative drift of these two oscillators over one day is a few times 10^{-13}. To reduce the long-term drift, which is principally due to excessive room temperature sensitivity, we have added cryogenic sensors for the power and frequency stabilization servos to one of these oscillators. We have also implemented a servo to reduce the room temperature sensitivity of our phase modulators. Testing of this oscillator against a Shanghai Observatory H-maser has shown an Allan deviation of 4$\times 10^{-15}$ from 600 to 2000 s.**

I. Introduction

In this paper, we report measurements of the properties of our new sapphire resonators which are strong determinants of oscillator stability, namely, the loaded Q and the frequency dependences of temperature and power. We will then focus on results of a stability comparison of two oscillators built around nominally identical resonators. Finally, we report improvements to the long-term stability of one of these oscillators and verification of this by comparison to a H-maser.

Oscillators displaying the level of stability demonstrated in this paper are required to satisfy the stringent needs for "flywheel" oscillators in the new generation of trapped ion atomic frequency standards. Excellent short-term stability has been shown by cryogenic oscillators with resonator quality factors in excess of 10^8 [1]–[4]. A microwave oscillator based on a 3-cm-diameter cryogenic sapphire dielectric resonator (SDR) with loaded Q-factor $\sim 10^8$ achieved a fractional frequency stability of 10^{-14} for integration times of 1–300 s [2]. The stability was chiefly limited by the frequency pulling effects of the external circuit. Since these effects and the frequency locking servo noise floor scale inversely as the Q-factor, improvements in oscillator stability are tied to improvements in Q-factor. Higher Q-factors are obtainable in the more highly confined modes of 5-cm-diameter resonators. We have previously measured $\sim 4\times 10^9$ at 4.2 K and 5–8$\times 10^9$ at 2 K [5] in resonators cut from Crystal Systems "HEMEX" material.

II. The Resonator

Two nominally identical resonators were cut from Crystal Systems "HEMEX" material and operated on an $H_{14\,1\,1}$ (quasi-$TE_{14\,1\,\delta}$) mode at 11.9 GHz, which displays a loaded Q of 10^9 at 6K. Each sapphire resonator is mounted inside a cylindrical niobium shield which is placed in a permanently evacuated vacuum pot. The pot was attached to a cryostat for cooling to liquid helium temperatures. Temperature control to a precision of about 10^{-5} K was provided by a Lake Shore DRC-91CA temperature controller using a carbon glass thermometer and a heater mounted in thermal contact with the shield.

Manuscript received July 1, 1994; revised October 15, 1994. This work was supported by the Australian Research Council.

The authors are with the Department of Physics, University of Western Australia, Nedlands, Western Australia, 6009 Australia.

IEEE Log Number 9408689.

A. Resonator Frequency-Temperature Dependence

Details of the two sapphire resonators have been presented elsewhere [6]. Resonator 1 was from a "white, high purity" boule and has a frequency maximum at 6 K described by a curvature $1/f\ d^2f/dT^2 \sim 10^{-9}\ \mathrm{K}^{-2}$. This frequency maximum considerably relaxes the temperature control requirement to permit $\sim 10^{-15}$ fractional frequency stability. Unfortunately, resonator 2 came from a "standard" boule, known to be slightly contaminated with titanium. This resonator has no extrema in our desired temperature range, but has a minimum slope of $3 \times 10^{-10}\ \mathrm{K}^{-1}$ at 6 K. The mode frequency temperature dependence of both resonators can be explained by a combination of the temperature dependence of the sapphire dielectric constant and the ac susceptibility of paramagnetic ions which have an electron spin resonance above 100 GHz [6]. The high confinement of field energy to the sapphire in the $H_{14\,1\,1}$ mode results in the superconducting shield having a negligible influence on the mode frequency.

B. Resonator Frequency-Power Dependence

In resonator 1, and at high power (>0.5 mW) in resonator 2, there is an approximate linear dependence of mode frequency on the microwave power dissipated in the resonator. The magnitude of $1/f\ df/dP$ is about $-10^{-10}\ \mathrm{mW}^{-1}$ for an unloaded Q of 2×10^9, which is consistent with the permittivity change due to electromagnetic radiation pressure quoted in [7]. This effect necessitates power level regulation to achieve long-term frequency stability below the 10^{-14} level.

III. Loop Oscillator

The improved loop oscillator circuit [3] is essentially our original configuration [2] with the addition of a power level servo and is shown in Fig. 1. In transmission, the resonator is the primary frequency determining element of the free-running loop oscillator, while in reflection it is the dispersive element in an active, Pound-type frequency stabilization scheme [8]. A bandpass filter ($Q \sim 10^3$) is necessary to select the required SDR mode. The circuit losses are compensated by the gain of the GaAs FET amplifier which runs in slight saturation. The

0018-9456/95$04.00 © 1995 IEEE

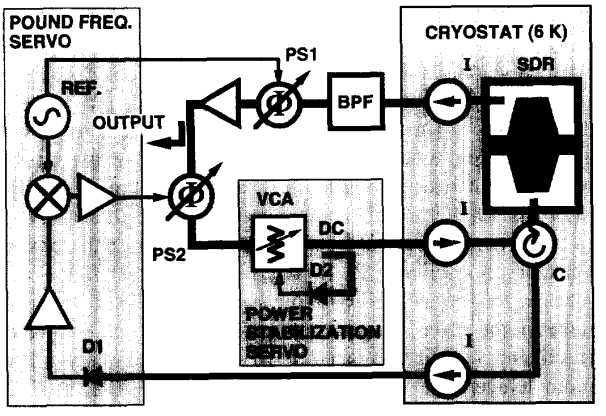

Fig. 1. The loop oscillator circuit.

loop electrical length is servo controlled by the Pound frequency stabilization scheme to lock the oscillation frequency to the centre of resonance. The carrier power incident on the SDR is phase modulated by a varactor diode phase shifter (PS1) driven by a crystal reference oscillator (at a rate of 1.4 MHz or 80 kHz) which is much larger than the resonator bandwidth. PM-to-AM conversion upon reflection provides the discriminator signal which is recovered by synchronous detection with the reference oscillator. The SDR input coupling is set near unity for maximum carrier suppression to permit square law operation of the detector diode (D1) and thereby maximize discriminator sensitivity. After amplification and filtering, the discriminator signal is fed back to a second varactor diode phase shifter (PS2) to control the frequency of the loop oscillator. The transfer function of the loop phase stabilization circuit is essentially that of a single integration and has a unity gain crossover point at about 1 kHz. We have operated one of the loop oscillators using a custom made low noise 1.4 MHz demodulation system and a commercial lock-in amplifier performing the same operation at 80 kHz. No difference in frequency stability was detected.

All of the loop oscillator components are at room temperature except for the circulator (C) and isolators (I) (typically 3 per transmission line) that are placed near the resonator to minimize frequency pulling effects. The microwave power dissipated in the resonator is typically 0.5 mW and is partially regulated by the power servo comprising the tunnel diode detector (D2) and voltage controlled attenuator (VCA). This servo fully compensates for amplifier power fluctuations and the variation of insertion loss of PS2 with the error voltage from the frequency stabilization servo. In oscillator 2 (based on resonator 2), D2 is at room temperature to allow for the power to be varied over a wide range to explore the mode frequency-power dependence. In oscillator 1 (based on resonator 1), D2 is instead placed near the resonator in the cryogenic environment. This eliminates both the long-term variation of incident power on the resonator due to variation of transmission line attenuation with liquid helium bath level and the temperature dependence of the detector sensitivity. In oscillator 1, D1 has also been placed near the resonator. This improves the noise floor of the frequency stabilization servo because of the elimination of the 5 dB transmission line loss before D1. By varying the coupling ratio of the directional coupler (DC) that provides power to D2, we can change the ratio of loop power to the fixed diode power. This allows us to trade off the noise floor of the power servo against the frequency stabilization servo noise floor in order to optimize the stability of the oscillator.

IV. Oscillator Stability

A. Measurement System

To evaluate oscillator performance, we have constructed two nominally identical systems, mounted in separate cryostats, and performed a standard two oscillator comparison using a double heterodyne configuration. The first difference frequency of 3.75 MHz (which is due to the slight dimensional mismatch between the resonators) is mixed with a similar frequency from a synthesizer that has less absolute instability. For time domain measurements longer than a few seconds, the synthesizer is locked to an HP5065A rubidium frequency standard and is set to generate a second difference frequency ~100 Hz which is then counted in a 300 Hz bandwidth on an HP5316A frequency counter. The noise floor of this method (C) is shown in Fig. 2. To circumvent this counter noise for measurement times under a few seconds, we use a "zero-beat" technique [4]. The method involves digitizing and recording the beat waveform of the two oscillators. It provides both the Allan deviation and the phase noise spectral density from the same measurements. The noise floor of this method (Z on Fig. 2) is about 2.5 times better than the conventional counter method.

B. Short-Term Stability

The oscillator stability (O), combining conventional frequency counter data and our "zero-beat" technique data, is shown in Fig. 2. A factor of $\sqrt{2}$ has been removed to display the Allan deviation due to a single oscillator, assuming equal instability in each. The noise floors of these measurements and estimates of various oscillator instabilities are also shown in Fig. 2. At short times, the Allan deviation appears to fall faster than τ^{-1} because of the bright line structure from vibrational modes in the resonator and power line frequency modulation. Above 0.2 s, it reaches an apparent floor of $3\text{–}4\times10^{-15}$, which extends to about 100 s. Amplifier flicker phase noise will be present in the oscillator output as it is coupled from the loop immediately after the amplifier. The observed stability below 0.1 s is consistent with amplifier flicker phase noise of $S_\phi \doteq -100/f$ dBc $\cdot$ Hz^{-1} which translates to an Allan deviation of approximately 5×10^{-16}/tau. The small rise in the Allan deviation around 2 s is due either to the 0.2 Hz beat between the two 1.4 MHz frequency stabilization servo reference oscillators, or to the oceanic microseism peak at 0.2 Hz which has an amplitude of up to 2×10^{-5} m$\cdot$s^{-2}. We had no accelerometers sensitive enough at 0.2 Hz to eliminate the latter possibility.

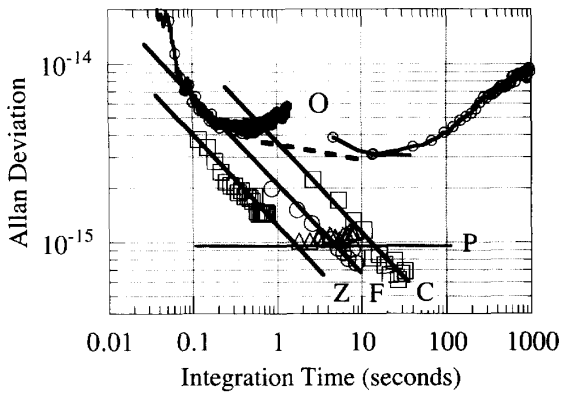

Fig. 2. Frequency stability of sapphire oscillator (O), noise floors of the measurement system (Z, C), and oscillator 2 servo systems (P, F).

We have measured the noise floors of the power and frequency control servo systems for oscillator 2 by placing an identical open loop servo system in parallel with the original, including a second detector that shares half of the microwave power of the original detector. The inferred Allan deviation due to the noise floor of the frequency control servo (F) improves as $1/\sqrt{\tau}$, as expected for the white frequency noise of the discriminator. The inferred Allan deviation due to the power servo (P) is flat, which is consistent with operation of the detector in its $1/f$ frequency regime. In preliminary measurements, the floor in oscillator 1 was much lower than that in oscillator 2, primarily due to the lower frequency versus power slope at the operating power in oscillator 1.

The above measurements show that the short-term stability is not limited by any of the servo systems, except between 0.07 and 0.2 s, where it appears to be limited by the frequency control servo on oscillator 2. The requirement for temperature stability in resonator 2 is very strict as its minimum slope is 3 $\mathrm{Hz \cdot K^{-1}}$. The oscillators' stability indicates that the resonator temperature stability must be much better than 10 μK, although we have been unable to verify this independently to better than 30 μK. Thus, temperature instability of resonator 2 has not been eliminated as a candidate. However, it would seem unlikely that temperature instability would dominate from 0.1 to 1000 s. The origin of our apparent flicker frequency floor is uncertain, although it may be due to intrinsic resonator flicker frequency noise. Frequency stability of the order of 10^{-15} is only realized with one other oscillator—the superconducting cavity maser [1], which also uses a cryogenic SDR and exhibits a similar flicker frequency floor from 1 to 1000 s. Ground vibration of order 10^{-5} $\mathrm{m \cdot s^{-2}}$ might also be significant in the short term since the phase noise below 1 Hz is partially correlated with accelerometers mounted on the cryostat and the acceleration sensitivity in resonator 1 appears to be a few times 10^{-8} $\mathrm{m \cdot s^{-2}}$.

The extreme level of short-term stability achieved by our oscillator could easily be transferred to an atomic frequency standard, using the intrinsic resonator power sensitivity to enable a low bandwidth frequency lock loop. The relatively large frequency-power coefficient gives the system adequate range to cope with long-term drifts of the sapphire oscillator.

C. Improvements in the Long-Term Stability

The addition of a power servo significantly improves the Allan deviation in the medium term although the performance in the long term still begins to degrade as approximately $3\times10^{-16}\tau^{1/2}$. The relative drift of the two oscillators over 1 day is a few times 10^{-13}, which is an order of magnitude improvement over the oscillators based on 3 cm resonators [2]. This long-term drift is dominated by the high sensitivity to room temperature (of about 5×10^{-13} $\mathrm{K^{-1}}$) of the power detector on oscillator 2. In order to better determine the intrinsic long-term stability of the sapphire oscillator, we have reduced the room temperature sensitivity on one oscillator (oscillator 1) and compared it to a hydrogen maser. The room temperature sensitivity was reduced to $\sim10^{-13}$ $\mathrm{K^{-1}}$ by employing cryogenic tunnel diode detectors for D1 and D2. The residual temperature sensitivity is then dominated by the reference phase modulator (PS1). Both phase modulators have a variation of insertion loss (IL) with bias level that causes incidental amplitude modulation (AM). Incidental AM due to the error signal in PS2 is removed by the power servo. However, the in-phase component of the AM from the reference signal in PS1 masquerades as a frequency offset error at the discriminator. In a few of our modulators, we find a turning point in the variation of IL with bias, which allows us to implement a servo to null the unwanted AM. A lock-in amplifier at the power servo detector (D2) recovers the in-phase component of the AM and provides an error signal for the bias of the phase modulator (PS1). With this AM servo system operating, the temperature sensitivity of oscillator 1 is less than $3\times10^{-14}\mathrm{K^{-1}}$.

D. Comparison to H-Maser

The sapphire oscillator was compared to a Shanghai Observatory H-maser model H-M12A. The stability of this maser has been previously determined against a Smithsonian VLG-10-1 maser [9], at 800 MHz. The sapphire oscillator is heterodyned with an HP8673H microwave synthesizer whose 5 MHz reference is phase locked to the 100 MHz output of the H-maser. Both the sapphire oscillator and H-M12A are housed in the same temperature controlled room, whose diurnal temperature fluctuations are less than 0.5 K. Temperature oscillations of 1 K amplitude with a typical period of 1600 s are due to the air-conditioner thermostat.

The stability measured over 13 h (triangles) is shown in Fig. 3, along with the results of the two maser intercomparison [9] (thick dotted line). We attribute the difference in the curves at small integration times to the poor phase noise of the maser quartz oscillator when multiplied to 11.9 GHz. The peculiar Allan deviation curve (triangles) shown in Fig. 3 arises from frequency modulation of the H-maser signal due to the modulation of room temperature. The magnitude of the frequency deviation is consistent with the maser sensing the room temperature oscillation filtered by a 90-min internal thermal time constant. The temperature coefficient of the H-maser is approximately 4×10^{-14} $\mathrm{K^{-1}}$. The frequency deviation could also be explained by assigning a room temperature sensitivity of 1×10^{-14} $\mathrm{K^{-1}}$ to the sapphire oscillator. Further work needs

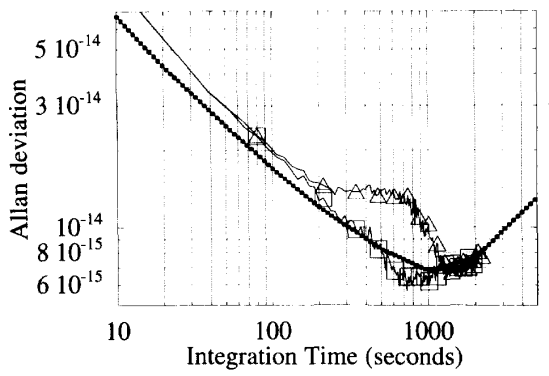

Fig. 3 . Comparison of Shanghai H-maser to: VLG-10-1 (thick dotted line), sapphire oscillator (triangles), and sapphire oscillator with effects of room temperature oscillation removed (squares).

to be done to isolate the source of the temperature sensitivity. By filtering out the temperature modulation from the data, we can obtain the result (squares) for a temperature stable measurement, which from 600 to 2000 s is less than or equal to the result of [9]. Taking into account the uncertainty in the Allan deviation at these integration times (50 data points), we arrive at an estimate of the instability associated with the sapphire oscillator of less than 4×10^{-15} from 600 to 2000 s.

V. Conclusions

We have demonstrated that a power, phase, AM, and temperature stabilized loop oscillator based on a cryogenic sapphire resonator can achieve fractional frequency stability of $3\text{–}4\times10^{-15}$ for integration times from 0.3 to 100 s and 4×10^{-15} from 600 to 2000 s. We have shown that the noise floors of the servo systems are not responsible for imposing the present flicker frequency floor. The origin of this floor is uncertain, although it may be due to intrinsic resonator flicker frequency noise. We have also shown that the long-term drift can be significantly reduced using cryogenic power servo detectors and by implementing a new AM servo system that reduces the effect of the temperature sensitivity of the phase modulators.

Acknowledgment

The authors thank W. Wilson of the Australia Telescope National Facility for providing us with data on the comparison of the Smithsonian and Shanghai Observatory H-masers. They also thank the ATNF and C. F. Lin and J. W. He of Shanghai Observatory for the loan of the H-maser.

References

[1] G. J. Dick and R. T. Wang, "Ultra-stable performance of the superconducting cavity maser," *IEEE Trans. Instrum. Meas.*, vol. 40, pp. 174–177, 1991.

[2] A. J. Giles, S. K. Jones, D. G. Blair, and M. J. Buckingham, "A high stability microwave oscillator based on a sapphire loaded superconducting cavity," *Proc. IEEE 43rd Ann. Freq. Contr. Symp.*, 1989, pp. 89–93.

[3] A. N. Luiten, A. G. Mann, and D. G. Blair, "Cryogenic sapphire microwave resonator-oscillator with exceptional stability," *Electron. Lett.*, vol. 30, pp. 417–419, 1994.

[4] M. E. Costa, A. N. Luiten, M. E. Tobar, and D. G. Blair, "Oscillator performance from the time evolution of relative phase," *Electron. Lett.*, vol. 30, pp. 149–151, 1994.

[5] A. N. Luiten, A. G. Mann, and D. G. Blair, "Ultra high Q factor cryogenic sapphire resonator," *Electron. Lett.*, vol. 29, pp. 879–881, 1993.

[6] ——, "Improved sapphire dielectric resonators for ultrastable oscillators," in *Proc. 47th Ann. Freq. Contr. Symp.*, Salt Lake City, UT, 1993, pp. 757–762.

[7] V. B. Braginskii, V. P. Mitrafanov, and V. I. Panov, *Systems with Small Dissipation.* Chicago: University of Chicago Press, 1985, p. 78.

[8] S. R. Stein and J. P. Turneaure, "The development of the superconducting cavity stabilized oscillator," in *Proc. 27th Ann. Freq. Contr. Symp.*, 1973, p. 414.

[9] W. E. Wilson, "Shanghai maser tests at Parkes," ATNF/CSIRO, Parkes, Australia, Jan. 1994.